# Investigations of optical properties of As$_2$S$_3$-Se nanomultilayers.

Vladimir ABASHKIN, Elena ACHIMOVA, Tezarii KRYSKOV, Alexei MESHALKIN, Alexander PRISACAR, Ghenadii TRIDUH Miroslav VLCEK[1]

*Institute of Applied Physics, Academy of Sciences of Moldova*
[1]*Department of General and Inorganic Chemistry, Faculty of Chemical Technology, University of Pardubice,*
*532 10 Pardubice, Czech Republic*
*achimova@phys.asm.md*

*Abstract* — **The chalcogenide glasses are interesting materials for investigation of nanostructural properties possessing unique characteristics which are different from those in oxide and halide glasses, i.e. molecular (low-dimensional) structures, semiconductor properties, including a wide range of optical transparency, high refractive index n and specific electrical resistance. The aim of the work is to extend the research of nanostructuring properties of As$_2$S$_3$-Se nanomultilayers meaning the possibilities of direct, one-step surface relief formation by laser beam. As$_2$S$_3$-Se nanomultilayers were prepared by thermal evaporation of two compositions from two isolated boats on constantly rotated substrate at room temperature in one vacuum deposition cycle. Two wide rings overlap in the central part of substrate forming nanostructure. Overlapping part of samples contains alternating nanolayers of Se and As$_2$S$_3$. Outside and internal rings of layers on the substrate contain pure compositions of Se and As$_2$S$_3$ consequently.**

**We present the study of photoinduced changes of optical properties of nanostructure As$_2$S$_3$-Se. On the base of the following parameters measured: optical transmittance and dispersion of refractive index we conclude that as-deposited nanostructures did not form solid solution from component material, but after illumination the photodiffution takes place.**

*Index Terms* — **Chalcogenide glasses, nanostructure formation, photo-structural transformation, photobleaching, interdiffusion, photodarkening.**

## I. INTRODUCTION

Nanostructure formation has been explored for many kinds of materials, and this becomes a promising topic also for glasses. At first in comparison with crystalline nanostructures the glassy nanostructure may yield a greater variety of compositions, since the bonding constraint arising from crystalline unit cells does not exist. The second reason is that the control of nanometer-scale structures could be an ultimate research subject for glassy structures.

Among the glasses, the chalcogenide glasses (ChG) are interesting materials for investigation of nanostructural properties possessing unique characteristics which are different from those in oxide and halide glasses, i.e. molecular (low-dimensional) structures, semiconductor properties, including a wide range of optical transparency, high refractive index n and specific electrical resistance.
ChG are versatile functional materials for optics, optoelectronics, and information technologies due to mainly the number of different photo-induced effects like photo-darkening and bleaching, local expansion or contraction, changes of the reflectivity and of the refraction index which take place in thin films of ChG [1–3].

In spite of the rather long history of such investigations the mechanisms of light-induced processes, structural transformations are still not completely clear.

Amorphous–amorphous or amorphous–crystalline structural transformations are the bases of optical recording, i.e. the formation of amplitude and phase optical reliefs [1, 3, 4]. The phase relief may be complemented by the change of the thickness, i.e. by geometrical surface relief formation directly during the optical recording or
by selective chemical etching. Few approaches are known for extending investigations of ChG towards the nanostructures, especially in the nanolayered, superlattice-like multilayer structures [3], but the problem of photo-
structural transformation (PST) dependence on the artificial nano-structuring is still not solved. The definition of nano-scale structures for ChG lies within 1–100nm. It is plausible that some properties vary with scale because of several reasons:

- the distinction among molecular, crystalline, and amorphous becomes vague;
- the fraction of atoms being located at surfaces or interfaces substantially rising respect to volume ones, which affect structure/optical properties;
- the mean free path of excitations is comparable to the structural scale, and accordingly, quantum-size effects may appear.

Inserting the photosensitive glass or just amorphous Se between the other ChG layers and changing the dimensions of this structure, new effects are expected further growth of the efficiency of volume expansion, stimulation of the solid-state chemical reactions, and crystallization.

The establishment of inter connections between the compositional modulation at nanoscaled dimensions (10–20nm) and the characteristics of optical recording were investigated. The aim of the work is to extend the

research of nanostructuring properties of $As_2S_3$-Se nanomultilayers meaning the possibilities of direct, one-step surface relief formation by laser beam.

## II. EXPERIMENTAL

The bulk samples of $As_2S_3$ and Se were synthesized by melt-quenching technique from elemental components which were heating in evacuated quartz ampoules at $T=900^oC$ during 30 hours.

ChG nanomultilayers were prepared by computer driven cyclic thermal vacuum deposition of two materials from two isolated boats on constantly rotated substrate at room temperature in one vacuum deposition cycle. The technology allows depositing thin films with thicknesses from 0.005 up to 3.0μm. The control of the thickness carried out during the thermal evaporation by interference thickness sensor at λ=0.95μm. Overlapping part of samples contains alternating nanolayers of Se and $As_2S_3$, i.e. two wide rings overlap in the central part of substrate forming nanostructure. Outside and internal rings of layers on the substrate contain pure compositions of Se and $As_2S_3$ consequently. Control layers of Se and $As_2S_3$ were deposited at the same time onto the same substrate consequently through masks and used to check the composition, and calculate the ratio of the sub-layer thicknesses in one modulation period. On the fig. 1 we present the photograph (fig. 1a) and cross-section (fig. 1b) of the samples.
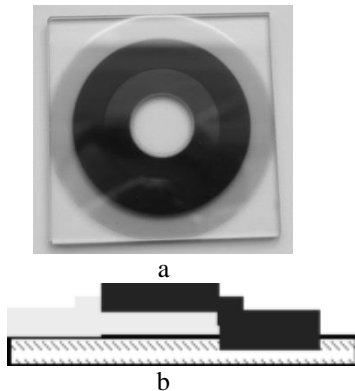


Fig. 1 The photograph (a) and cross-section (b) of $As_2S_3$-Se nanostructure.

Resulting samples were $As_2S_3$-Se type structures with total thickness 2–3 μm, the modulation periods (the total thickness of one $As_2S_3$ and one Se nanolayers) 20–50 nm range and the wide band-gap material $As_2S_3$ was the optically transparent barrier and the active material Se had a narrower band-gap.

PST were induced by DPSS green laser radiation (λ=0.53μm) with output intensities 30mW. Optical parameters (optical transmission spectra and the change of them under illumination) were recorded on two-beam spectrophotometer SPECORDM40 in the range of wave lengths of 200–900nm.

## III. RESULTS AND DISCUSSION

The examination of the transmission spectra of $As_2S_3$-Se nanostructure showed that the samples have good thickness uniformity proved by the existence of many interference peaks as for separated $As_2S_3$ and Se layers as

for total $As_2S_3$-Se nanostructure (fig. 2, 3). This fact allows us to calculate the thickness and refractive index of layers by Swanepoel method. There is broad transparency region at long wavelengths and significant drop of transparency in the region of 400-600 nm due to the increase of absorption. The transmission spectra for $As_2S_3$-Se nanostructure with modulation period 50nm presented on the fig. 2 are similar the spectra on the fig. 3 for modulation period 25nm. The absorption edges for $As_2S_3$ and Se layers are in accordance with well known data for these materials [3]. Note that the edge of absorption spectra of $As_2S_3$-Se nanostructure coincides with edge of absorption spectra of Se layer, which is narrower band gap material. It is expected result, but the absence of shift of the absorption edge of nanostructure to wider band gap material ($As_2S_3$) indicates the inter-diffusion between $As_2S_3$ and Se does not take place.
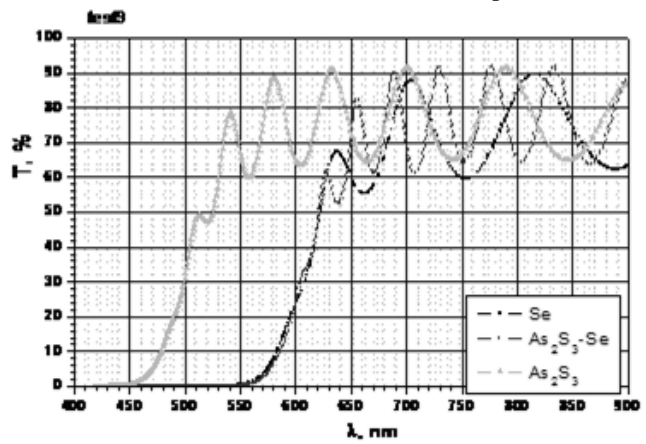


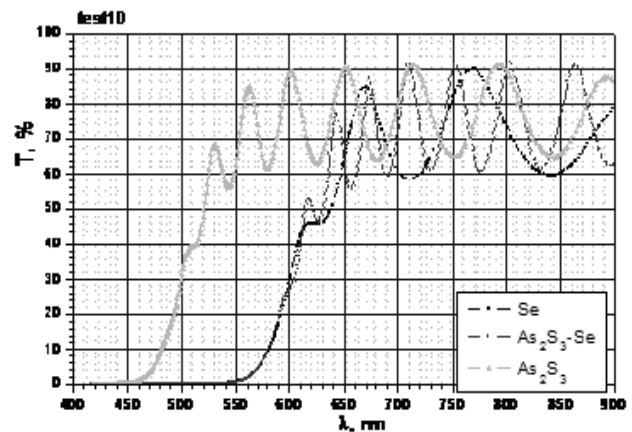Fig. 2 The transmission spectra of $As_2S_3$-Se nanostructure with modulation period 50nm.



Fig. 3 The transmission spectra of $As_2S_3$-Se nanostructure with modulation period 50nm.

In the analysis of optical transmission spectra the "effective optical medium" model [2] has been applied in which mainly the "well" layers, with small $E_{gv}$ energy, determine the optical absorption $\alpha = 10^2$-$10^5$ cm$^{-1}$ at the average absorption edge $E_g$, and the "barrier" layers with larger $E_{gb}$ are transparent. Since in this model the absorption is mainly determined by the "well" layers, the relation:

$$\alpha hv = const \ (hv - E_g)^2$$

can be used for the determination of $E_g$ in amorphous semiconductors, where hv is the energy of light quantum.

During laser irradiation photo-bleaching (blue shift of absorption edge) in $As_2S_3$-Se nanostructure has been observed, as it was usual for this type of nanostructures [1, 3]. One of the possible explanations of this blue shift given by authors [5] consists in interdiffusion, taking place between components of structure. The advantage of induced interdiffusion of more- and less-absorptive layers in such a layered, chalcogenide-based structure consists in the creation of solid solutions with a changed optical absorption edge. Irradiation by laser light with wavelength which corresponds to the optical band gap of the matrix material ($\lambda$=532nm in our case, where the light penetrates all sub-layers and the absorption is still rather efficient), induces interdiffusion. Here laser exposure leads to solid state synthesis of a two component materials $As_2S_3$ and Se from initially separated nanolayers. There action causes a blue shift (Fig.4) of the overall optical absorption edge of the nanostructured medium to the edge of the $As_2S_3$ component glass at the end of the process.
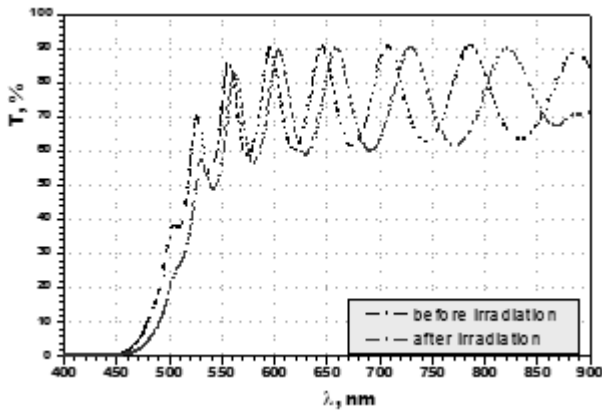


Fig. 4 The transmission spectra of $As_2S_3$-Se nanostructure before and after irradiation.
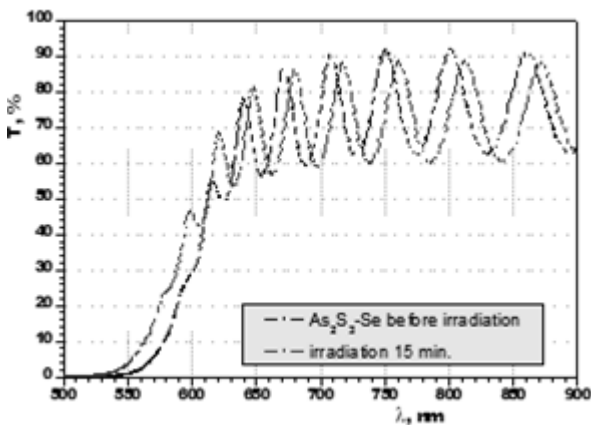


Fig. 5 The transmission spectra of $As_2S_3$ films before and after irradiation.

The observed blue-shift is $\Delta \lambda = 0.20$nm. It is interesting that for $As_2S_3$ the shift of optical absorption edge moves towards longer wavelengths so called red shift (see fig. 5 for illustration).

In this case ($As_2S_3$) photodarkening is about 10nm, which is typical for arsenic sulfide material under illumination [5].

From the optical transmission spectra the optical band gap $E_g$ was also determined. It can be obtained from Tauc law:

$$(\alpha\hbar\omega)^{1/2} = f(E)$$

In paper [3] it was stated that for the present type of materials one should prefer Tauc law in contrast with using dependence $\alpha = f(E)$. In fig. 6 energy dependence of $(\alpha E)^{1/2}$
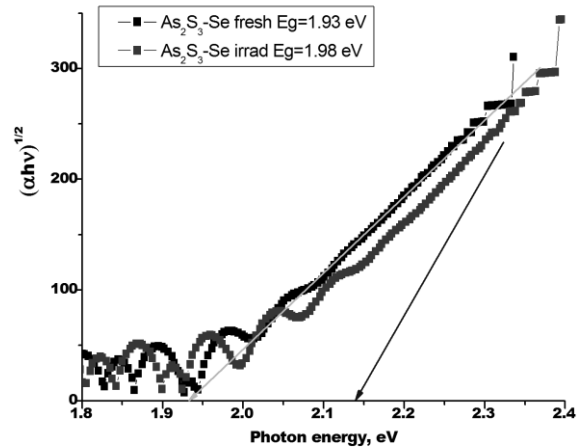


Fig.6 Determination of optical band gap $E_g$ from Tauc plot.

parameter is plotted. Linear range in the region of high photon energies corresponds to the Tauc law. Energy band gap is the point where this line intersects with abscissa (see fig. 6).

Spectral dependence of refractive index calculated together with films thickness by Swanepoel method [4] is given in the fig. 7. According the Swanepoel method the spectral dependence of refractive index describes by the function:
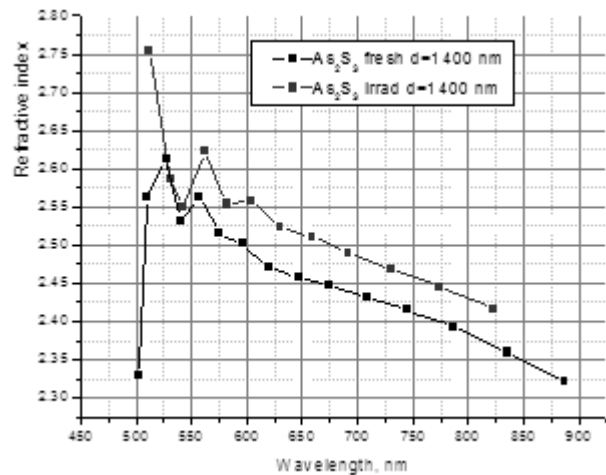


$$n(\lambda) = a/\lambda^2 + c$$

Fig. 7 The spectral dependence of refractive index of $As_2S_3$ films before and after irradiation.

From fig. 7 one can see that the refractive index of $As_2S_3$ films changes from 2.6 up to 2.35 in spectral range 500-850 nm. The irradiation increases refractive index on 0.25 in the same domain.

The dispersion of refractive index of $As_2S_3$-Se nanostructure is less pronounced ($\Delta n = 0.15$) and practically has not change under irradiation (see fig. 8).
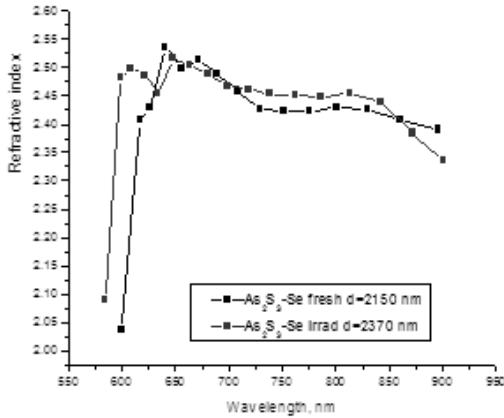
Fig. 8 The spectral dependence of refractive index of As$_2$S$_3$-Se nanostructure before and after irradiation.

The following figures 9 and 10 present dispersion of refractive index for two types of As$_2$S$_3$-Se nanostructure: modulation period 25nm (fig. 9) and 50nm (fig. 10).
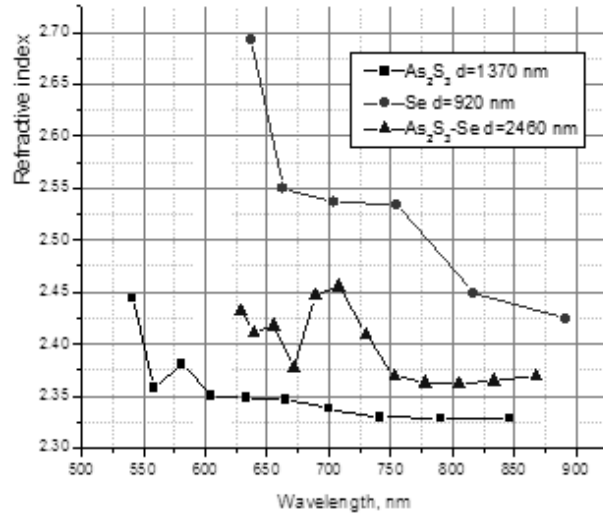


Fig. 9 The spectral dependence of refractive index of As$_2$S$_3$, Se films and As$_2$S$_3$-Se nanostructure with modulation period 25nm.

For modulation period 25nm the refractive index of As$_2$S$_3$-Se nanostructure is more than it of As$_2$S$_3$ ($\Delta n$ = 0.15÷0.25), and lies between refractive indexes of individual films of As$_2$S$_3$ and Se (Fig. 9).

The As$_2$S$_3$-Se nanostructure with modulation period 50nm exhibits different behavior. This characteristic lies close to one belonging to As$_2$S$_3$ films, and within the experimental error refractive index of nanostructure does not change (see fig. 10).

If we propose that interdiffusion between As$_2$S$_3$ and Se mono-nano layers takes place that the decreasing of modulation period leads to increasing the probability of penetration one material, most likelihood is Se, into As$_2$S$_3$.

## IV. CONCLUSION

Optical properties of the As$_2$S$_3$-Se nanostructure were investigated. It was shown that as-deposited nanostructures did not form solid solution from component material, but after illumination the photodiffution takes place.

## REFERENCES

[1] M. Popescu, A. Andries, V. Ciumas, M. Iovu, S. Sutov, D. Tciuleanu, in: Fizica sticelor calcogenice (Eds.), Stiintifica, Bucuresti, 1996.

[2] P. Berning, in „Physics of Thin Films", ed. H. Hasse, Moscow, Mir (1967)

[6] Е. Ф. Венгер, А. В. Мельничук, А. В. Стронский. Фотостимулированные процессы в халькогенидных полупроводниках. Киев, 2007.

[7] R. Swanepoel, J. Phys. E: Sci. Instrum. 16, 1214 (1983).

[8] A. Csik, A. Kikineshi, D. L. Beke, I. A. Szabo, and G. Langer, J. Optoelectronics and Advanced Materials 3, 33 (2001)

Fig. 10 The spectral dependence of refractive index of As$_2$S$_3$, Se and As$_2$S$_3$-Se nanostructure with period 50nm.